This is an open access article published under a Creative Commons Attribution (CC-BY) License, which permits unrestricted use, distribution and reproduction in any medium, provided the author and source are cited.

ACS OMEGA

Article

Cite This: ACS Omega 2019, 4, 19614−19622

http://pubs.acs.org/journal/acsodf

Polymeric Core−Shell Combinatorial Nanomedicine for Synergistic Anticancer Therapy

Asifkhan Shanavas,*[,†] Nishant K. Jain,[‡] Navneet Kaur,[†] Dinesh Thummuri,[∥,⊥] Maruthi Prasanna,[‡] Rajendra Prasad,[‡] Vegi Ganga Modi Naidu,[∥] Dhirendra Bahadur,*[,§,#] and Rohit Srivastava*[,‡]

[†]Habitat Centre, Institute of Nano Science and Technology, Phase-X, Sector-64, Mohali, Punjab 160062, India

[‡]Department of Biosciences and Bioengineering and [§]Department of Metallurgical Engineering & Materials Science, Indian Institute of Technology Bombay, Powai, Mumbai 400076, India

[∥]National Institute of Pharmaceutical Education and Research Guwahati, Nits Mirza Road, Parlli Part, Guwahati Assam 781125, India

Supporting Information

ABSTRACT: Core−shell nanostructures are promising platforms for combination drug delivery. However, their complicated synthesis process, poor stability, surface engineering, and low biocompatibility are major hurdles. Herein, a carboxymethyl chitosan-coated poly(lactide-*co*-glycolide) (cmcPLGA) core−shell nanostructure is prepared via a simple one-step nanoprecipitation self-assembly process. Engineered core−shell nanostructures are tested for combination delivery of loaded docetaxel and doxorubicin in a cancer-mimicked environment. The drugs are compartmentalized in a shell (doxorubicin, Dox) and a core (docetaxel, Dtxl) with loading contents of ∼1.2 and ∼2.06%, respectively. Carboxymethyl chitosan with both amine and carboxyl groups act as a polyampholyte in diminishing ζ-potential of nanoparticles from fairly negative (−13 mV) to near neutral (−2 mV) while moving from a physiological pH (7.4) to an acidic tumor pH (6) that can help the nanoparticles to accumulate and release the drug on-site. The dual-drug formulation was found to carry a clinically comparable 1.7:1 weight ratio of Dtxl/Dox, nanoengineered for the sequential release of Dox followed by Dtxl. Single and engineered combinatorial nanoformulations show better growth inhibition toward three different cancer cells compared to free drug treatment. Importantly, Dox−Dtxl cmcPLGA nanoparticles scored synergism with combination index values between 0.2 and 0.3 in BT549 (breast ductal carcinoma), PC3 (prostate cancer), and A549 (lung adenocarcinoma) cell lines, demonstrating significant cell growth inhibition at lower drug concentrations as compared to single-drug control groups. The observed promising performance of dual-drug formulation is due to the G2/M phase arrest and apoptosis.

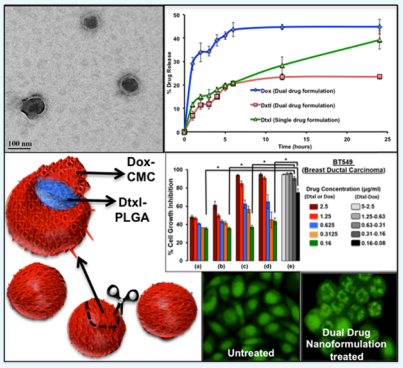

INTRODUCTION

Cancer is a notorious disorder that can find loopholes in its basic molecular mechanisms to bypass various signaling pathways, which are hit by small molecule therapeutics. This is one of the ways to evolve toward prolonged survival and metastasis.[1] Cancer chemoresistance is due to the increased expression of P-glycoprotein (Pgp) drug efflux pumps, enhanced drug metabolism, or altered structure of the drug targets.[2] Combination chemotherapy plays a crucial role in cancer treatment due to rising concerns over resistance to single-drug regimen over the course of time.[3] This approach limits the cancer cells to undergo mutational changes needed for cancer cell adaptation and can invoke synergism between the drugs to increase therapeutic efficiency and target selectivity.[4] Due to variations in pharmacokinetics, membrane transport, and biodistribution properties of different chemotherapeutics, dosage and optimization of drug scheduling become highly difficult.[5] Additionally, with more drugs added to the combination module, risks of side effects increase. Nanoengineering can spatially isolate and encapsulate multiple therapeutics at the same time to deliver them simultaneously or sequentially according to various physiological or external stimuli.[6,7] While codelivery of different single-drug-loaded nanoparticles is possible, importance needs to be given to multidrug-containing particles as they offer vehicle uniformity and ratiometric drug loading with a temporal release of the drugs. There are various reports on multidrug delivery using nanoparticles that showed promise in both in vitro and preclinical stages,[8,9] liposomes are considered as an ideal drug delivery platform for stimuli-responsive targeted drug delivery applications.[10] So far, several liposomal formulations of drugs such as doxorubicin (Doxil), daunorubicin (DaunoXome), cytarabine (DepoCyt), and vincristine (ONCO-TCS) have been marketed successfully. Due to their vesicular structure, they can load hydrophobic drugs in their unilamellar or multilamellar walls and a hydrophilic drug in their aqueous

Received: July 13, 2019
Accepted: October 4, 2019
Published: November 11, 2019

© 2019 American Chemical Society

DOI: 10.1021/acsomega.9b02167
ACS Omega 2019, 4, 19614−19622

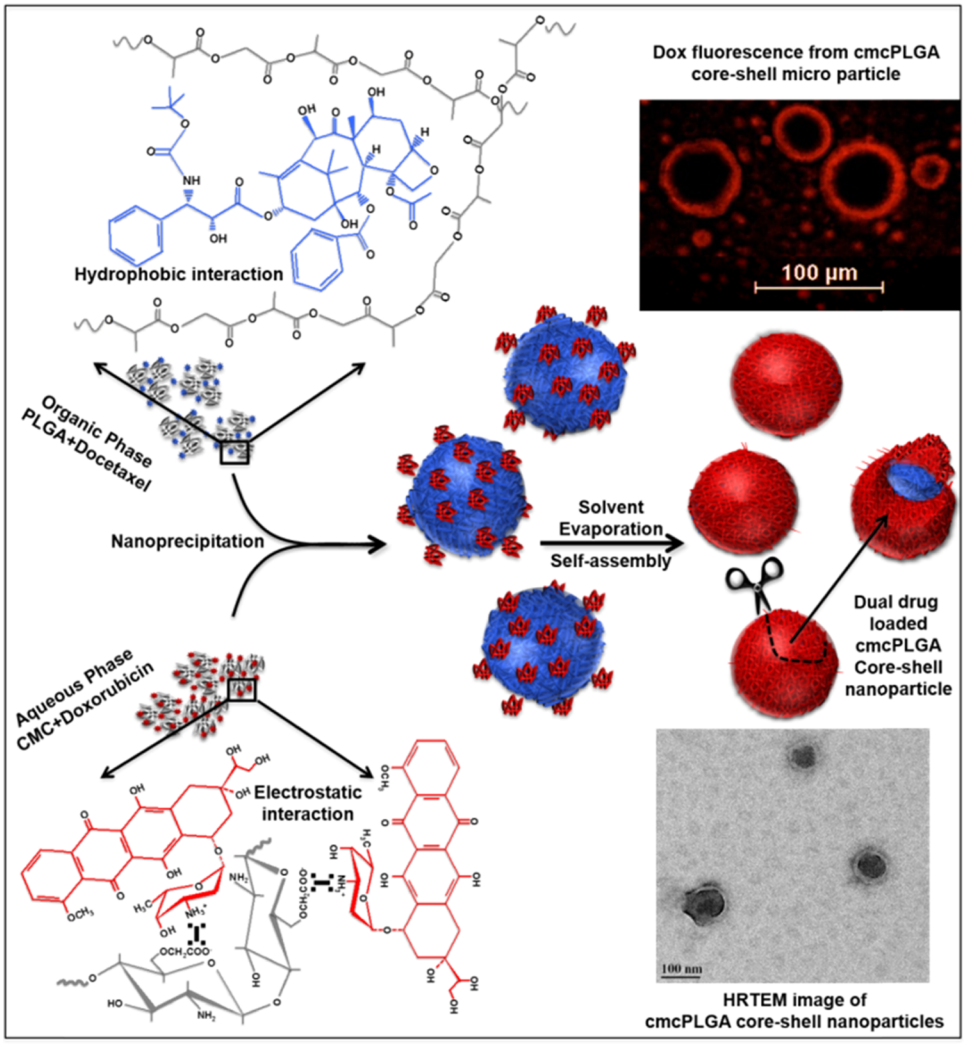

Figure 1. Schematic illustration showing fabrication of cmcPLGA core−shell nanoparticles via nanoprecipitation followed by solvent evaporation and electrostatic interaction induced self-assembly process.

core. However, poor stability and fragile structure are the major limitations of liposome-based nanoplatforms.[10,11] Alternatively, polymer-based nanoparticles have been utilized as promising platforms for drug delivery applications due to their predominant stability, low size polydispersity, tunable physicochemical properties, and better loading capacity for poorly water-soluble drugs.[7,12] Coencapsulation of drugs in polymeric nanoparticles is possible by directly loading water-insoluble molecules in the hydrophobic core, compartmentalizing the core by incorporating a "shell" on the surface for loading a hydrophilic/hydrophobic drug combination, or covalently conjugating different drugs in the polymer chain backbone. A recent work showed the encapsulation of a hydrophobic drug docetaxel in the core with a hydrophilic polymer covalently attached on the surface of doxorubicin.[13] While coencapsulation in the core has little control over the release pattern of the structurally and chemically different drugs, compartmentalized encapsulation provide the option of temporal control with simultaneous or sequential release of the drugs. A recent work validates a compartmentalized drug delivery carrier, where the core is made up of a self-assembled starch-based polymer encapsulating apogossypolone, an anticancer resistance drug, and the shell is decorated with hyaluronic acid nanoparticle loaded with doxorubicin, both associated electrostatically.[14] In another report, hydrophobic combretastatin A4 and the hydrophilic doxorubicin drugs are encapsulated separately in the core and shell of poly(vinylpyrrolidone)/poly(lactic/glycolic acid) (PVP/PLGA) and poly(ε-caprolactone) (PCL)/PLGA nanoparticles.[15] While there are other promising reports in recent years on simple yet effective combinatorial nanomedicines,[16−27] it is imperative to fabricate a novel multidrug nanoformulation that can compartmentalize small molecules during a facile synthesis procedure that can be easily scaled up.

The present work explores the pH-dependent surface charge switching carboxymethyl chitosan (CMC)-coated PLGA (cmcPLGA) core−shell nanoparticles encapsulating doxorubicin in the shell and docetaxel in the core prepared using a facile one-pot nanoprecipitation cum self-assembly process. The typical synthesis of cmcPLGA nanoparticle is shown schematically in Figure 1. The method involves in situ formation of core−shell morphology and compartmentalized docetaxel (Dtxl) and doxorubicin (Dox) loading. The drug loading is driven by hydrophobic interactions between Dtxl and PLGA, while Dox and CMC interact electrostatically. Figure 1 also clearly shows the encapsulation of Dox in a cmcPLGA core−shell microparticle, which is otherwise difficult to be visualized in the nanoregime.

DOI: 10.1021/acsomega.9b02167
ACS Omega 2019, 4, 19614−19622

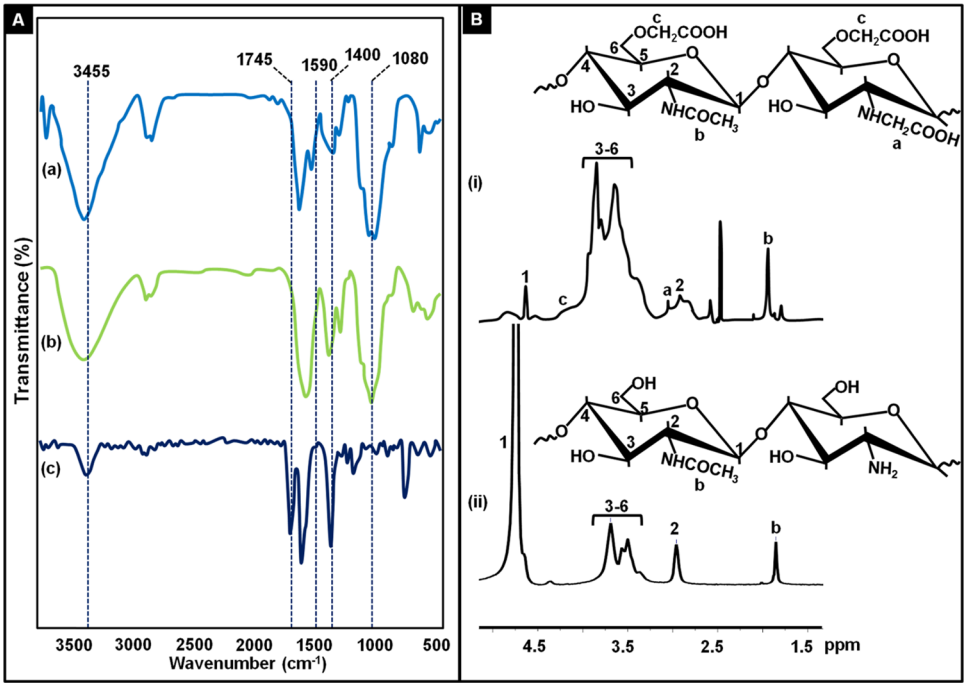

Figure 2. (A) FTIR spectra of chitosan (a), carboxymethyl chitosan (b), and monochloroacetic acid (c). (B) ^{1}H NMR spectra of carboxymethyl chitosan (i) and chitosan (ii) with respective structures.

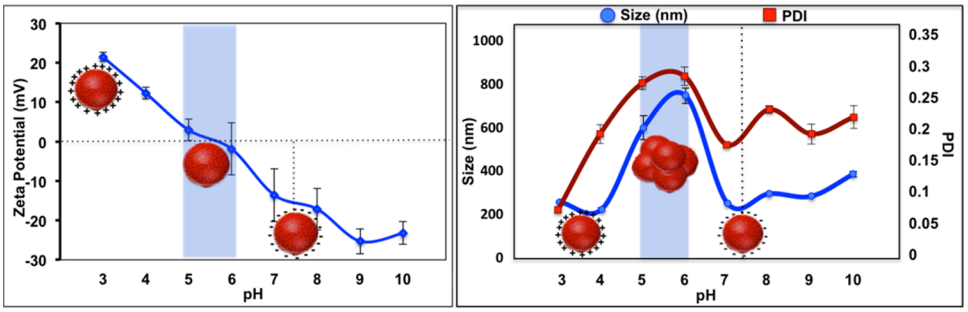

Figure 3. Hydrodynamic size, polydispersity index (PDI), and ζ-potential of blank cmcPLGA nanoparticles at varying pH conditions. The blue highlighted area shows the pH range where the isoelectric point of the nanoparticles lies.

RESULTS AND DISCUSSION

Rationale for CarboxyMethyl Chitosan as a Shell. Chitosan in its unmodified form was initially explored to serve as a shell on a PLGA nanoparticle due to its positive charge, and it could enhance cellular uptake due to the charge effect.[28] However, the main purpose of loading a second drug in the shell was not achieved due to a very less doxorubicin encapsulation efficiency of only ∼5%. The main reason could be due to an irregular coating throughout the sample, which is carried out after the PLGA nanoparticle synthesis, causing undesirable nanoparticle aggregation. It was hypothesized that the problem can be solved if the coating is carried out in situ during PLGA nanoprecipitation; yet, chitosan could not be used due to its poor aqueous solubility and the further instability of the PLGA nanodroplets formed if the process was performed in an acidic pH. To address this issue, a water-soluble form of chitosan is required to be used. Carboxymethyl chitosan (CMC) is a well-warranted polymer that has been widely studied because of its ease of synthesis, cost effectiveness, and ampholytic character possessing both cationic (amine) and anionic (carboxyl) functional groups that has made researchers exploring it as a drug delivery carrier and hydrogel in tissue engineering.[29] CMC can be synthesized in various forms predominantly as N,O-CMC or O-CMC, with "O" and "N" representing the hydroxyl substitution and amine substitution with the carboxymethyl group, respectively. The current work needed as many amine groups intact as possible for the electrostatic interaction of CMC with the anionic surface of PLGA nanodroplets during the synthesis process.

Characterization of Carboxymethyl Chitosan. Prior to nanoparticle preparation, the as-synthesized carboxymethyl chitosan was first characterized using Fourier transform infrared (FTIR) and ^{1}H NMR spectroscopy techniques. FTIR spectra shown in Figure 2A depict peaks at 1080 cm^{-1} corresponding to the glycosidic bond C−O−C and C−O stretching. The peak at 1400 cm^{-1} corresponds to carboxymethyl group, and the peak at 1745 cm^{-1} indicates the carboxyl group. The broad peak at 3455 cm^{-1} is due to the axial stretching of O−H and N−H bonds in chitosan.

The ^{1}H NMR spectrum of CMC (Figure 2B) in D_2O at 300 MHz shows a chemical shift at δ1.9, which corresponds to protons of the acetamido group ($NHCOCH_3$) in chitosan. Broad resonance between 4 and 4.5 ppm corresponds to protons of O−CH_2COOD.[22] The appearance of a new signal

DOI: 10.1021/acsomega.9b02167
ACS Omega 2019, 4, 19614−19622

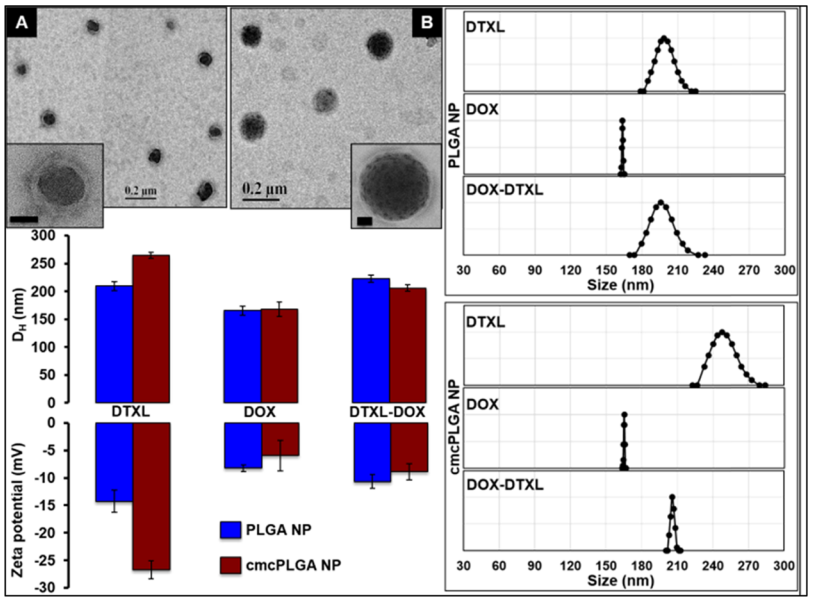

Figure 4. TEM images of Dox−Dtxl (A) and Dtxl (B) loaded cmcPLGA nanoparticles (inset scale bar, 20 nm). Hydrodynamic diameter, intensity-weighted size distribution, and ζ-potential measurements of single- and dual-drug formulations.

at 3 ppm corresponds to protons from the NH−CH_2COOD group between 3 and 3.5 ppm, which means the partial presence of N,O-CMC in the polymer.[30]

Morphology and Surface Chemistry of the Shell. To evaluate the stability of the blank nanoparticles, dynamic light scattering and ζ-potential measurements were recorded at varying pH values. Due to its ampholytic nature, carboxymethyl chitosan displayed a positive surface charge in the acidic medium owing to the protonation of amine groups and a negative charge at near-neutral and alkaline media due to deprotonation at amine and carboxyl groups. The isoelectric point was found to lie between 5 and 6, with significant particle instability found in this range, as observed from the increased size (600−750 nm) and high polydispersity index (PDI) due to aggregation with ζ-potential values from −3 to +2 mV, as shown in Figure 3. This near-neutral charge of the nanoparticles at a pH range of 5.5−6 can significantly influence the preferential adherence due to the partial presence of amine groups followed by accumulation and drug release in an acidic tumor microenvironment.[31]

Fabrication of Dual-Drug-Loaded Nanoformulations. The blank core−shell cmcPLGA nanoparticles synthesized were about 80 nm in size, with a shell width of ∼5 nm as observed by transmission electron microscopy TEM) analysis, as shown in Figure S2. The hydrodynamic size was measured to be about 200 nm. The dual-drug-loaded nanoparticles also showed a core−shell morphology in TEM analysis with a size of ∼100 nm (Figure 4).

Drug loading significantly affected the PLGA nanoparticle size when compared to that of blank nanoparticles, as shown in Figure S3. Among three different drugs analyzed for encasing in the core, docetaxel showed better encapsulation (∼94%) compared to that of tamoxifen citrate (∼15%) and doxorubicin (∼17.5%) due to its proven hydrophobic interaction with PLGA.[32] Doxorubicin, when loaded into the shell, caused a reduction in the hydrodynamic size and ζ-potential of the final core−shell nanoparticle at pH 7.4, from 250 to 200 nm and −16.7 to −8.88 mV, respectively (Figure 4). A simultaneous reduction in size and ζ-potential in the presence of Dox could be related to the compaction effect provided by the Dox-CMC shell and the positively charged Dox, masking the negative carboxyl groups of CMC. The charge masking effect of Dox is in line with a previous report, which showed conjugation of the drug with hyaluronic acid, flipping the surface charge from negative to positive.[14] Size reduction also decreased the encapsulation efficiency of Dtxl to ∼65% (Table 1) in the presence of Dox.

Table 1. Dual-Drug Encapsulation and Loading Efficiency

	encapsulation efficiency (%)		loading content (%)	
formulation	Dox	Dtxl	Dox	Dtxl
Dox F	55 ± 25.1		1.62 ± 0.01	
Dtxl F		94 ± 15.3		3.28 ± 0.13
Dox−Dtxl F	50 ± 9.2	65 ± 12.08	1.2 ± 0.03	2.06 ± 0.09

While a previous work has reported Dox-loaded CMC nanoparticles for nanodrug delivery,[33] in the present work it is vital to optimize the CMC concentration at which better Dox loading is possible in the shell of the nanoparticles. An increase in Dox encapsulation (∼55%) with the increase in CMC concentration up to 0.25% w/v was observed, beyond which the nanoparticle yield reduced drastically, adversely affecting the drug loading as can be seen in Figure 5.

A higher Dox loading was noted in the presence of CMC (∼1.2% with Dtxl and ∼1.6% without Dtxl) compared to the Dox loading in the absence of CMC (∼0.5% with Dtxl and ∼0.7% without Dtxl), as shown in Figure 5B, due to the electrostatic interaction of more Dox molecules with CMC. Dox loading seen in the absence of CMC is due to its interaction with carboxyl and hydrophobic functional groups in the superficial layers of PLGA that can also occur in the presence of CMC, aiding better loading.

Drug Release Kinetics. A sequential drug release was observed with a faster Dox release than Dtxl owing to its presence in the shell with a lesser resistance from CMC, smaller distance to diffuse out, and hydrophilicity that help in moving toward the aqueous medium at pH 7.4. Both the drugs

DOI: 10.1021/acsomega.9b02167
ACS Omega 2019, 4, 19614−19622

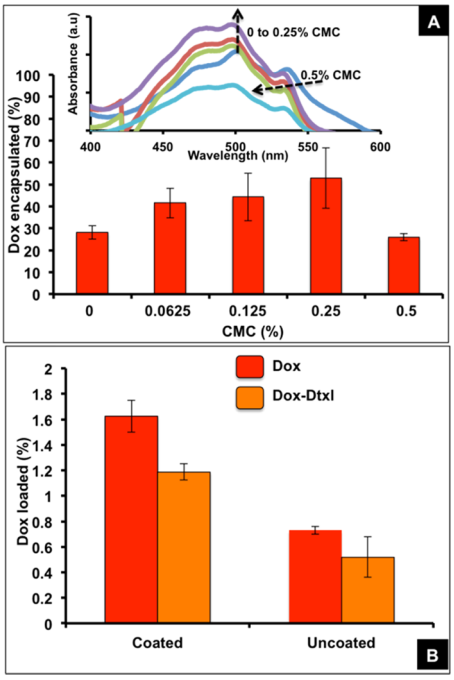

Figure 5. Percent Dox encapsulation under different CMC concentrations (A) (inset, UV−visible spectra of Dox extracted from the nanoparticles prepared with different weight percentages of CMC). Percent Dox loading with and without the CMC coating (B).

showed a biphasic release pattern with a burst within the first hour followed by a short saturation with a lagged release till sixth hour after which it reached a steady state (Figure 6). The

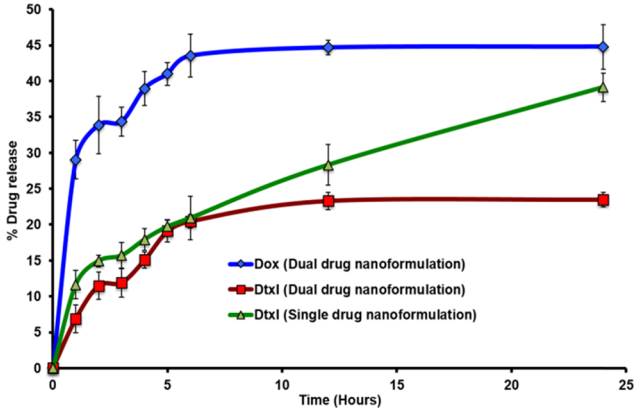

Figure 6. Drug release pattern from single- and dual-drug-loaded cmcPLGA nanoparticles.

second saturation was not observed in the case of Dtxl when loaded as a single drug in the nanoparticles, possibly due to the absence of resistance from the electrostatically cross-linked Dox-CMC shell. This resistance is also expected to limit the overall release of both the drugs in the dual-drug formulation under normal physiological conditions. The presence of ∼80% of Dtxl and ∼55% of Dox in the nanoparticle at the end of 24 h provides for the release of the remaining cargo after being uptaken by the cancer cells.

Engineered Nanoformulation for Cancer Cell Growth Inhibition. The effect of single- and dual-drug formulations was assessed in three different cell lines, viz., BT549 (breast ductal carcinoma), PC3 (prostate cancer), and A549 (lung adenocarcinoma), each being different in their tissue of origin. These cell lines were selected to observe the toxicity of formulation on the basis of the proliferation index of the cells. Both cancer cell lines BT549 and PC3 are indicated in opposite sexes, female and male, respectively, with closer proliferation indexes of 2.3 and 2.1.[34,35] The A549 cancer cells are indicated as common for both sexes with a proliferation index of 1.1,[36] which is about half of the other two cell lines. The dual-drug formulation was found to carry ∼1.7:1 weight ratio of Dtxl/Dox at the optimized conditions nanoengineered for a sequential release of Dox followed by Dtxl. The clinically correlated ratio ranges from 1.2:1 to 1.5:1, depending upon study objectives with sequential administration of Dox followed by Dtxl in metastatic breast cancer patients.[37,38] The core−shell nanoparticles showed time-dependant uptake in cancer cells with significant accumulation in the cytoplasm at the end of 6 h incubation (Figure S4). The free drug response at end of 48 h incubation was found to differ for each of the cell lines with BT459 requiring a maximum free Dox concentration of about 1.934 μg/mL (3.56 μM) to reach IC50 (Figure 7) followed by PC3 (1.812 μg/mL; 3.33 μM) and A549 (0.253 μg/mL; 0.465 μM). In the case of free Dtxl, A549 showed a cytostatic effect scoring the maximum IC50 of 5.716 μg/mL (7.09 μM) followed by a dose-dependent growth inhibitory effect for both BT549 and PC3 with IC50 values of 1.15 and 0.266 μM, respectively. Nanoformulations showed better growth inhibition compared to that of free drug formulations. While single-drug nanoformulation had a prominent effect at higher concentrations, dual-drug nanoformulation showed significant cell growth inhibition even at lower drug concentrations, mainly due to their synergistic effect (Figure 7). The IC50 values of the dual-drug formulation were found to be as low as 5 ng/mL (Dox equivalent, 9.2 nM) and 7 ng/mL (Dtxl equivalent, 8.68 nM) in A549 cell line. As expected, the IC50 values were higher in BT549 (Dox equivalent, 44.23 nM and Dtxl equivalent, 62 nM) and PC3 (Dox equivalent, 22 nM and Dtxl equivalent, 33.5 nM) cells owing to their high proliferation index. The combination Index that predicts whether a two-drug therapeutic regime follows synergism (C.I. < 1), additive (C.I. = 1), or antagonism (C.I. > 1) showed synergism in the case of Dox−Dtxl cmcPLGA nanoparticles with values between 0.2 and 0.3 for all of the three cell lines (Table 2). A comparative chart of Dox and Dtxl IC50 values in the three cell lines with the previously reported values is tabulated in Table S1.

Acridine orange and Ethidium bromide (AO/EtBr) Staining and Cell Cycle Analysis. Acridine orange and ethidium bromide (AO/EtBr) staining of PC3 prostate cancer cells showed chromatin breakdown, as can be seen in Figure 8, a characteristic feature of apoptosis, and it was prominent in cells treated with the dual-drug formulation (Dox, 50 ng/mL; Dtxl, 100 ng/mL) than cells treated with free and single-drug formulations, each at a concentration of 100 ng/mL. Our results clearly showed that Dox augmented the cytotoxic effects of Dtxl, which was further validated by cell cycle analysis. Dtxl and Dox are known to inhibit the cell cycle at the G2/M phase.[39,40] Dox−Dtxl combination formulation profoundly (>80%) inhibited the cells at the G2/M phase compared to single-drug formulations (Figure 9).

CONCLUSIONS

We report nanoparticles made of a PLGA core and a carboxymethyl chitosan shell with a pH-specific change in

DOI: 10.1021/acsomega.9b02167
ACS Omega 2019, 4, 19614−19622

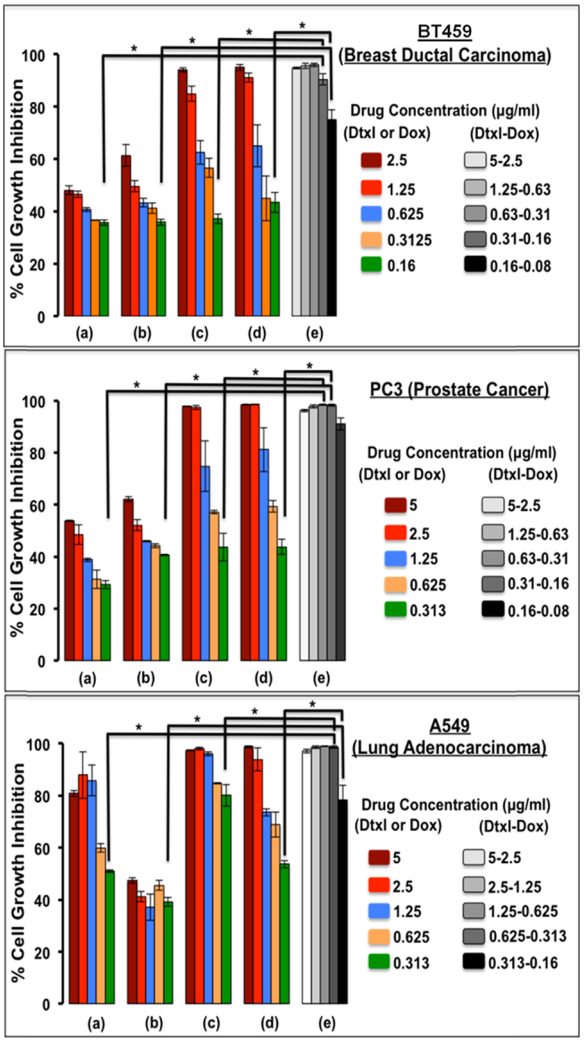

Figure 7. Dual-drug cell inhibitory effect of dual-drug-loaded cmcPLGA nanoparticles (e) on BT549, PC3, and A549 cancer cell lines as compared with that of free drug (a, Dox; b, Dtxl) and single-drug (c, Dox-cmcPLGA; d, Dtxl cmcPLGA) formulations at 48 h. *Two-tailed p value <0.01.

surface charge and compartmentalized dual-drug loading using a one-pot synthesis procedure. Nanoparticle characterization showed visible CMC coating with Dtxl (core) and Dox (shell) encapsulation of 94 and 55%, respectively. Due to the polyampholytic nature of CMC, the synthesized core−shell nanoparticles were found to have a positive and negative surface charge at acidic and alkaline pH values, respectively, with the isoelectric point lying between pH values of 5 and 6. The drug release profile showed a sequential release of Dox followed by Dtxl at physiological pH (7.4). The cell growth inhibitory effect of dual-drug formulation was significantly higher than that of free drug and single-drug nanoformulations. The combination drug delivery showed synergism between the two drugs, thus proving efficient than the control groups. While herein we report a combinatorial nanomedicine, the potential of the technology to fabricate layered microparticles to serve as postsurgical local implants for controlled sequential drug delivery cannot be ruled out. In both cases, a comprehensive in vivo study would fetch more light to establish the efficiency of the combination drug delivery in preclinical tumor models.

EXPERIMENTAL SECTION

Chemicals and Reagents. Chitosan (medium molecular weight), docetaxel, doxorubicin hydrochloride, 3-(4,5-dimethylthiazol-2-yl)-2,5-diphenyltetrazolium bromide (MTT), acridine orange, propidium iodide, and ethidium bromide were purchased from Sigma-Aldrich Ltd. PLGA (17 kDa, 50:50) was provided by PURAC Biomaterials. Monochloroacetic acid and polyvinyl alcohol were purchased from S.D. Fine Chemicals Ltd. RNAse A was purchased from Invitrogen. Cell lines PC3 and A549 were procured from NCCS, and BT549 was a gift sample from CCMB. Dialysis membrane, fetal bovine serum (FBS), DMEM, RPMI1640, penicillin−streptavidin solution, and trypsin EDTA were purchased from HiMedia Ltd. All solvents used were of analytical grade.

Synthesis of CarboxyMethyl Chitosan. The synthesis of CMC was as per protocol reported by Zhu et al.[29] Chitosan (8% w/v) was immersed in 25 mL of NaOH (50% w/v) solution to swell for 24 h. The alkalized chitosan was crushed into a filtration cake and then transferred into a flask. Five grams of monochloroacetic acid was dissolved in 25 mL of isopropanol and then added to the flask dropwise for 20 min. The reaction in the flask was allowed to continue for 8 h at room temperature, after which the mixture was filtered to remove the solvent. The filtrate obtained was dissolved in 100 mL of water, and 2.5 M HCl was added to it to adjust its pH to ∼7. Following pH adjustments, anhydrous ethanol was added to precipitate the product that is further centrifuged to remove the precipitate. Finally, the product was filtered, rinsed thrice with anhydrous ethanol, and vacuum-dried at room temperature.

Synthesis of Dual-Drug loaded Carboxymethyl chitosan-Coated PLGA (cmcPLGA) Nanoparticles. The core−shell nanoparticles was prepared using a single-step nanoprecipitation self-assembly process by slowly adding 5 mL of organic phase (tetrahydrofuran) containing 5 mg/mL PLGA (17 kDa, 50:50) and docetaxel (10% w/w of PLGA) into 10 mL of aqueous mixture containing previously synthesized carboxymethyl chitosan (0.25% w/v), doxorubicin hydrochloride (10% w/w of CMC), and PVA (2% w/v) under vigorous stirring followed by solvent evaporation at room temperature. After complete solvent evaporation, the nanoparticles were separated from excess PVA by centrifugation at 15 000 rpm for 30 min and further washed once with double distilled water at 15 000 rpm for 10 min. The nanoparticles

Table 2. IC50 Values (ng/mL) of Single- and Dual-Drug Formulations for Three Different Cancer Cell Lines

					Dtxl−Dox formulation		
cancer type	Dox solution	Dtxl solution	Dox formulation	Dtxl formulation	Dox equivalent*	Dtxl equivalent*	C.I.#
A549	253 ± 6	5716 ± 597	134 ± 14	236 ± 16	5 ± 3	7 ± 5	0.27
BT459	1934 ± 78	928 ± 45	264 ± 19	349 ± 107	24 ± 10	50 ± 21	0.24
PC3	1812 ± 197	215 ± 6	917 ± 82	204 ± 20	12 ± 3	27 ± 10	0.2

DOI: 10.1021/acsomega.9b02167
ACS Omega 2019, 4, 19614−19622

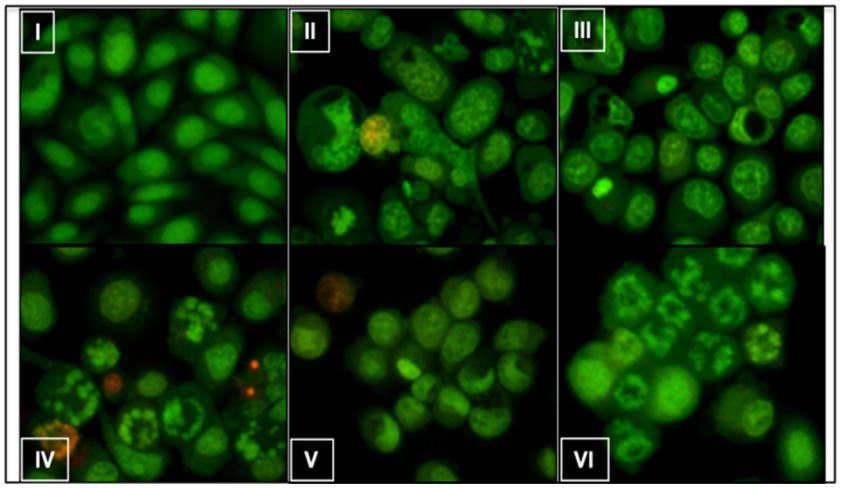

Figure 8. Determination of morophlogical changes by acridine orange/ethidium bromide staining. (I) Untreated, (II) Dox 100 ng/mL, (III) Dtxl 100 ng/mL, (IV) Dox formulation 100 ng/mL, (V) Dtxl formulation 100 ng/mL, and (VI) Dox−Dtxl formulation 50−100 ng/mL treated PC3 cells for 24 h showing various degrees of apoptotic chromatin breakdown.

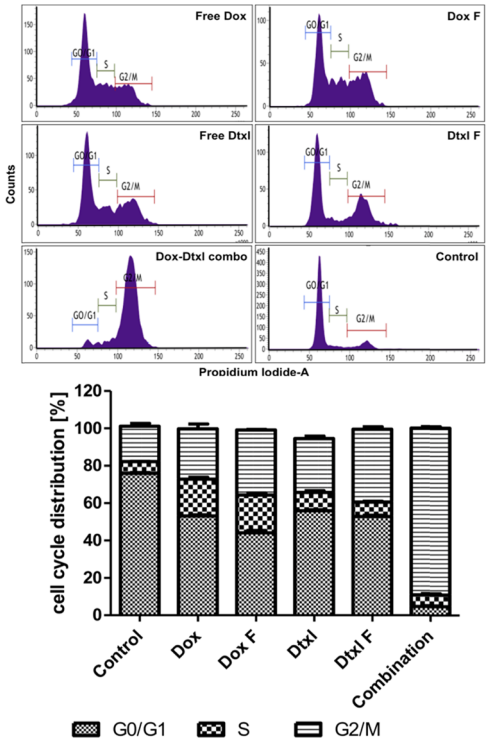

Figure 9. Flow cytometric analyses of PC3 cells treated with free Dox (100 ng/mL), free Dtxl (100 ng/mL), Dox formulation (100 ng/mL), Dtxl formulation (100 ng/mL), and Dox−Dtxl formulation (50−100 ng/mL) for 24 h.

were dispersed in double distilled water at 1 mg/mL concentration prior to freeze-drying and stored at 4 °C until further use.

Drug Encapsulation and Loading Studies. A known quantity of Dox−Dtxl-loaded nanoparticles were dispersed in water−acetonitrile mixture and left for drug dissolution into the solution phase under constant shaking overnight. The mixture was centrifuged to remove polymer debris, and the supernatant was analyzed using high-performance liquid chromatography (HPLC) for doxorubicin and docetaxel absorbance at λ_{max} of 230 nm with retention times of 6.06 and 7.118 min, respectively (Figure S1). This method was used to directly measure the amount of the drug loaded in the particles. The EE (encapsulation efficiency) and LC (loading content) of drugs were calculated using the following formulas

$$\text{EE (\%)} = \frac{\text{weight of drug encapsulated}}{\text{weight of drug in feed}} \times 100$$

$$\text{LC (\%)} = \frac{\text{weight of drug loaded}}{\text{weight of nanoformulation}} \times 100$$

Drug Release Study. The dual-drug release study from cmcPLGA nanoparticles was performed by a dialysis membrane method for the samples against 1% Tween 80 in phosphate-buffered saline (pH 7.4) at 37 °C. Predetermined quantities of aliquots were taken from the release medium at regular time intervals and replaced with an equal volume of fresh buffer to maintain constant sink conditions. The aliquots were quantified for both docetaxel and doxorubicin using HPLC as mentioned earlier. The measurements were performed in triplicate for calculating mean ± standard deviation.

Cell Growth Inhibition Studies. To elucidate the effect of unloaded and Dox−Dtxl-loaded cmcPLGA nanoparticles on cancer cells, the MTT assay was performed according to the method reported by Mallavadhani et al.[41] A549 and PC3 cells were cultured in RPMI1640, and BT549 cells were cultured in DMEM. Culture media were supplemented with 10% fetal bovine serum, penicillin, and streptomycin. Briefly, A549, PC3, and BT549 cells were seeded at a density of 1×10^4 cells per well in a 96-well plate containing 10% FBS. After 24 h, cells were treated with different concentrations of free drug, dual-drug, and single-drug nanoformulations for a period of 48 h. At the end of incubation, 10 μL of MTT (5 mg/mL) in 100 μL medium was added and incubated at 37 °C for 4 h. Then, the media with MTT was removed and the purple formazan crystals formed were dissolved in 200 μL of dimethyl sulphoxide and read at 570 nm using a multidetection plate reader (SpectraMax M4, Molecular Devices, USA). The cell inhibitory efficiency and dual-drug combination index were calculated as follows

DOI: 10.1021/acsomega.9b02167
ACS Omega 2019, 4, 19614−19622

$$\text{cell growth inhibition (\%)} = \left[1 - \frac{A_{\text{sample}}}{A_{\text{control}}}\right] \times 100$$

where A_{sample} and $A_{control}$ are absorbance values of nanoparticle-treated and untreated cells, respectively.

$$\text{combination index (C. I)} = \frac{D_1}{D_{50a}} + \frac{D_2}{D_{50b}}$$

where D_1 and D_2 are drug concentration of Dox and Dtxl, respectively, and D_{50a} and D_{50b} are 50% inhibitory concentration (IC50) values of Dox formulation and Dtxl formulation, respectively.

Acridine orange and Ethidium bromide (AO/EtBr). AO/EtBr staining was performed for imaging apoptotic chromatin breakdown in treated cells according to the method reported by Mallavadhani et al.[41] PC3 cells were grown in 6-well plates for 24 h followed by treatment with the samples for 24 h. After the incubation period, the cells were fixed with 1% glutaraldehyde for 30 min and observed under a inverted fluorescence microscope with the help of a digital camera (Nikon, Inc. 246 Japan) at 200X magnification.

Cell Cycle Analysis. To determine the effect of Dox, Dtxl, and Dox−Dtxl formulations on cell cycle analysis, 24 h after plating 1×10^6 PC3 cells on 6-well plates, cells were incubated with free drug, single, and combination formulations for 24 h. Thereafter, cells were washed in phosphate-buffered saline, trypsinzed, and fixed in 70% alcohol. After fixing, RNAse A (1 mg/mL) and PI (10 mg/mL) were added to each sample. Samples were incubated at room temperature in complete darkness for 30 min. Cell cycle distribution was determined using BD fluorescence-activated cell sorting (FACS) verse. The results were analyzed by BD FACSuite software.

Statistical Analysis. An unpaired student's *t*-test (two-tailed) with confidence intervals of 99% and 95% was taken for analysis using Graph Pad software. The groups compared are indicated as necessary.

■ ASSOCIATED CONTENT

Supporting Information

The Supporting Information is available free of charge on the ACS Publications website at DOI: 10.1021/acsomega.9b02167.

Nanoparticle characterization methods; HPLC chromatogram of doxorubicin and docetaxel; scanning electron microscopy images of blank nanoparticles; nanoparticle cellular uptake; and tabulation of doxorubicin and docetaxel IC50 values (PDF)

■ AUTHOR INFORMATION

Corresponding Authors

*E-mail: asifkhan@inst.ac.in (A.S.).
*E-mail: dhirendra@iitgoa.ac.in (D.B.).
*E-mail: rsrivasta@iitb.ac.in (R.S.).

ORCID

Asifkhan Shanavas: 0000-0001-7221-7477
Rajendra Prasad: 0000-0001-9851-8630
Dhirendra Bahadur: 0000-0002-5092-6624
Rohit Srivastava: 0000-0002-3937-5139

Present Addresses

#Department of Mechanical Engineering, Indian Institute of Technology Goa, Goa College of Engineering Campus, Farmagudi, Ponda-403401, Goa (D.B.)
⊥University of Florida, Department of Pharmacodynamics, 1333 center drive basic sciences building, Gainesville, FL, USA 32610 (D.T.)

Notes

The authors declare no competing financial interest.

■ ACKNOWLEDGMENTS

The authors would like to acknowledge the Department of Science and Technology, Government of India for funding under the SERB-EMR scheme (EMR/2016/003851). The authors also thank Corbion Purac Biomaterials, Netherlands for providing a complimentary PLGA sample.

■ REFERENCES

(1) Derakhshan, A.; Chen, Z.; Van Waes, C. Therapeutic Small Molecules Target Inhibitor of Apoptosis Proteins in Cancers with Deregulation of Extrinsic and Intrinsic Cell Death Pathways. *Clin. Cancer Res.* 2017, DOI: 10.1158/1078-0432.CCR-16-2172.

(2) Waghray, D.; Zhang, Q. Inhibit or Evade Multidrug Resistance P-Glycoprotein in Cancer Treatment. *J. Med. Chem.*. 2018, DOI: 10.1021/acs.jmedchem.7b01457.

(3) Che-Ming, J.; Santosh, A.; Liangfang, Z. Nanoparticle-Assisted Combination Therapies for Effective Cancer Treatment. *Ther. Deliv.* 2010. https://doi.org/10.4155/tde.10.13.

(4) Lehár, J.; Krueger, A. S.; Avery, W.; Heilbut, A. M.; Johansen, L. M.; Price, E. R.; Rickles, R. J.; Short, G. F.; Staunton, J. E.; Jin, X.; et al. Synergistic Drug Combinations Tend to Improve Therapeutically Relevant Selectivity. *Nat. Biotechnol.* 2009. https://doi.org/10.1038/nbt.1549.

(5) van De Waterbeemd, H.; Smith, D. A.; Beaumont, K.; Walker, D. K. Property-Based Design: Optimization of Drug Absorption and Pharmacokinetics. *J. Med. Chem.* **2001**, DOI: 10.1021/jm000407e.

(6) Español, L.; Larrea, A.; Andreu, V.; Mendoza, G.; Arruebo, M.; Sebastian, V.; Aurora-Prado, M. S.; Kedor-Hackmann, E. R. M.; Santoro, M. I. R. M.; Santamaria, J. Dual Encapsulation of Hydrophobic and Hydrophilic Drugs in PLGA Nanoparticles by a Single-Step Method: Drug Delivery and Cytotoxicity Assays. *RSC Adv.* 2016, DOI: 10.1039/C6RA23620K.

(7) Aryal, S.; Hu, C. M. J.; Zhang, L. Polymeric Nanoparticles with Precise Ratiometric Control over Drug Loading for Combination Therapy. *Mol. Pharmaceutics*. 2011, DOI: 10.1021/mp200243k.

(8) Agrawal, V.; Paul, M. K.; Mukhopadhyay, A. K. 6-Mercaptopurine and Daunorubicin Double Drug Liposomes - Preparation, Drug-Drug Interaction and Characterization. *J. Liposome Res.* 2005, DOI: 10.1080/08982100500364081.

(9) Mayer, L. D. Ratiometric Dosing of Anticancer Drug Combinations: Controlling Drug Ratios after Systemic Administration Regulates Therapeutic Activity in Tumor-Bearing Mice. *Mol. Cancer Ther.* 2006. , DOI: 10.1158/1535-7163.MCT-06-0118.

(10) Sharma, A. U. S. Liposomes in drug delivery: progress and limitations. *Int. J. Pharm.* **1997**, *154*, 123−140.

(11) Lee, S.-M.; Nguyen, S. T. Smart Nanoscale Drug Delivery Platforms from Stimuli-Responsive Polymers and Liposomes. 2013, DOI: 10.1021/ma401529w.

(12) Kamaly, N.; Yameen, B.; Wu, J.; Farokhzad, O. C. Degradable Controlled-Release Polymers and Polymeric Nanoparticles: Mechanisms of Controlling Drug Release. *Chem. Rev.* 2016, DOI: 10.1021/acs.chemrev.5b00346.

(13) Jäger, E.; Jäger, A.; Chytil, P.; Etrych, T.; Říhová, B.; Giacomelli, F. C.; Štěpánek, P.; Ulbrich, K. Combination Chemotherapy Using Core-Shell Nanoparticles through the Self-Assembly of HPMA-Based Copolymers and Degradable Polyester. *J. Control. Release* 2013, DOI: 10.1016/j.jconrel.2012.11.009.

DOI: 10.1021/acsomega.9b02167
ACS Omega 2019, 4, 19614−19622

(14) Li, K.; Liu, H.; Gao, W.; Chen, M.; Zeng, Y.; Liu, J.; Xu, L.; Wu, D. Mulberry-like Dual-Drug Complicated Nanocarriers Assembled with Apogossypolone Amphiphilic Starch Micelles and Doxorubicin Hyaluronic Acid Nanoparticles for Tumor Combination and Targeted Therapy. *Biomaterials* 2015, DOI: 10.1016/j.biomaterials.2014.10.073.
(15) Cao, Y.; Wang, B.; Wang, Y.; Lou, D. Polymer-Controlled Core-Shell Nanoparticles: A Novel Strategy for Sequential Drug Release. *RSC Adv.* 2014, DOI: 10.1039/C4RA03610G.
(16) Chandran, P.; Gupta, N.; Retnakumari, A. P.; Malarvizhi, G. L.; Keechilat, P.; Nair, S.; Koyakutty, M. Simultaneous Inhibition of Aberrant Cancer Kinome Using Rationally Designed Polymer-Protein Core-Shell Nanomedicine. *Nanomedicine Nanotechnology, Biol. Med.* 2013, DOI: 10.1016/j.nano.2013.04.012.
(17) Malarvizhi, G. L.; Retnakumari, A. P.; Nair, S.; Koyakutty, M. Transferrin Targeted Core-Shell Nanomedicine for Combinatorial Delivery of Doxorubicin and Sorafenib against Hepatocellular Carcinoma. *Nanomedicine Nanotechnology, Biol. Med.* 2014, DOI: 10.1016/j.nano.2014.05.011.
(18) Malarvizhi, G. L.; Chandran, P.; Retnakumari, A. P.; Ramachandran, R.; Gupta, N.; Nair, S.; Koyakutty, M. A Rationally Designed Photo-Chemo Core-Shell Nanomedicine for Inhibiting the Migration of Metastatic Breast Cancer Cells Followed by Photodynamic Killing. *Nanomedicine Nanotechnology, Biol. Med.* 2014, DOI: 10.1016/j.nano.2013.10.006.
(19) Narayanan, S.; Mony, U.; Vijaykumar, D. K.; Koyakutty, M.; Paul-Prasanth, B.; Menon, D. Sequential Release of Epigallocatechin Gallate and Paclitaxel from PLGA-Casein Core/Shell Nanoparticles Sensitizes Drug-Resistant Breast Cancer Cells. *Nanomedicine Nanotechnology, Biol. Med.* 2015, DOI: 10.1016/j.nano.2015.03.015.
(20) Zhao, Y.; Huan, M.; Liu, M.; Cheng, Y.; Sun, Y.; Cui, H.; Liu, D.-Z.; Mei, Q.-B.; Zhou, S.-Y. Doxorubicin and resveratrol co-delivery nanoparticle to overcome doxorubicin resistance. *Scientific Reports* **2016**, DOI: 10.1038/srep35267.
(21) Menon, J. U.; Kuriakose, A.; Iyer, R.; Hernandez, E.; Gandee, L.; Zhang, S.; Takahashi, M.; Zhang, Z.; Saha, D.; Nguyen, K. T. Dual-Drug Containing Core-Shell Nanoparticles for Lung Cancer Therapy. *Sci. Rep.* 2017, DOI: 10.1038/s41598-017-13320-4.
(22) Lee, Y. H.; Chang, D. S. Fabrication, characterization, and biological evaluation of anti-HER2 indocyanine green-doxorubicin-encapsulated PEG-b-PLGA copolymeric nanoparticles for targeted photochemotherapy of breast cancer cells. *Scientific Reports* **2017**, DOI: 10.1038/srep46688.
(23) Shahbazi, M.; Almeida, P. V.; Correia, A.; Herranz-Blanco, B.; Shrestha, N.; Mäkilä, E.; Salonen, J.; Hirvonen, J.; Santos, H. A. Intracellular responsive dual delivery by endosomolytic polyplexes carrying DNA anchored porous silicon nanoparticles *J. Control. Release* 2017 DOI: 10.1016/j.jconrel.2017.01.046.
(24) Farooq, M. U.; Novosad, V.; Rozhkova, E. A.; Wali, H.; Ali, A.; Fateh, A. A.; Neogi, P. B.; Neogi, A.; Wang, Z. Gold Nanoparticles-enabled Efficient Dual Delivery of Anticancer Therapeutics to HeLa Cells. *Scientific Reports* **2018**, DOI: 10.1038/s41598-018-21331-y.
(25) Gupta, P. K.; Pappuru, S.; Gupta, S.; Patra, B.; Chakraborty, D.; Verma, R. S. Self-Assembled Dual-Drug Loaded Core-Shell Nanoparticles Based on Metal-Free Fully Alternating Polyester for Cancer Theranostics. *Mater. Sci. Eng. C* 2019, DOI: 10.1016/j.msec.2019.03.041.
(26) Zhang, L.; Zhu, H.; Gu, Y.; Wang, X.; Wu, P. Dual drug-loaded PLA nanoparticles bypassing drug resistance for improved leukemia therapy *J. Nanoparticle Res* 2019 DOI: 10.1007/s11051-018-4430-0.
(27) Jiang, S.; Wang, K.; Dai, Y.; Zhang, X.; Xia, F. Near-Infrared Light-Triggered Dual Drug Release Using Gold Nanorod-Embedded Thermosensitive Nanogel-Crosslinked Hydrogels *Macromol. Mater. Eng.* 2019 DOI: 10.1002/mame.201900087.
(28) Yang, R.; Yang, S. G.; Shim, W. S.; Cui, F.; Cheng, G.; Kim, I. W.; Kim, D. D.; Chung, S. J.; Shim, C. K. Lung-Specific Delivery of Paclitaxel by Chitosan-Modified PLGA Nanoparticles via Transient Formation of Microaggregates. *J. Pharm. Sci.* 2009, DOI: 10.1002/jps.21487.
(29) Aiping, Z.; Jianhong, L.; Wenhui, Y. Effective Loading and Controlled Release of Camptothecin by O-Carboxymethylchitosan Aggregates. *Carbohydr. Polym.* 2006, DOI: 10.1016/j.carbpol.2005.08.006.
(30) Mourya, V. K.; Inamdar, N. N.; Tiwari, A. Carboxymethyl Chitosan and Its Applications. *Advanced Materials Letters*. 2010. https://doi.org/10.5185/amlett.2010.3108.
(31) Tannock, I. F.; Rotin, D. Acid PH in Tumors and Its Potential for Therapeutic Exploitation. *Cancer Res.* **1989**, *49*, 4373−4384.
(32) Musumeci, T.; Ventura, C. A.; Giannone, I.; Ruozi, B.; Montenegro, L.; Pignatello, R.; Puglisi, G. PLA/PLGA Nanoparticles for Sustained Release of Docetaxel. *Int. J. Pharm.* 2006, DOI: 10.1016/j.ijpharm.2006.06.023.
(33) Sahu, S. K.; Mallick, S. K.; Santra, S.; Maiti, T. K.; Ghosh, S. K.; Pramanik, P. In Vitro Evaluation of Folic Acid Modified Carboxymethyl Chitosan Nanoparticles Loaded with Doxorubicin for Targeted Delivery. *J. Mater. Sci. Mater. Med.* **2010**, *21*, 1587−1597.
(34) Kenny, P. A.; Lee, G. Y.; Myers, C. A.; Neve, R. M.; Semeiks, J. R.; Spellman, P. T.; Lorenz, K.; Lee, E. H.; Barcellos-Hoff, M. H.; Petersen, O. W.; et al. The Morphologies of Breast Cancer Cell Lines in Three-Dimensional Assays Correlate with Their Profiles of Gene Expression. *Mol. Oncol.* 2007, DOI: 10.1016/j.molonc.2007.02.004.
(35) Wang, Z.-H.; Hsu, H.-W.; Chou, J.-C.; Yu, C.-H.; Bau, D.-T.; Wang, G.-J.; Huang, C.-Y.; Wang, P. S.; Wang, S.-W. Cytotoxic Effect of S-Petasin and Iso-s-Petasin on the Proliferation of Human Prostate Cancer Cells. *Anticancer Res.* **2015**, *35*, 191−199.
(36) Ding, X.-Y.; Ding, J.; Wu, K.; Wen, W.; Liu, C.; Yan, H.-X.; Chen, C.; Wang, S.; Tang, H.; Gao, C.-K.; et al. Cross-Talk between Endothelial Cells and Tumor via Delta-like Ligand 4/Notch/PTEN Signaling Inhibits Lung Cancer Growth. *Oncogene* **2012**, *31*, 2899−2906.
(37) Misset, J. L.; Dieras, V.; Gruia, G.; Bourgeois, H.; Cvitkovic, E.; Kalla, S.; Bozec, L.; Beuzeboc, P.; Jasmin, C.; Aussel, J. P.; et al. Dose-Finding Study of Docetaxel and Doxorubicin in First-Line Treatment of Patients with Metastatic Breast Cancer. *Ann. Oncol. Off. J. Eur. Soc. Med. Oncol.* **1999**, *10*, 553−560.
(38) Itoh, K.; Sasaki, Y.; Fujii, H.; Minami, H.; Ohtsu, T.; Wakita, H.; Igarashi, T.; Watanabe, Y.; Onozawa, Y.; Kashimura, M.; et al. Study of Dose Escalation and Sequence Switching of Administration of the Combination of Docetaxel and Doxorubicin in Advanced Breast Cancer. *Clin. Cancer Res.* **2000**, *6*, 4082−4090.
(39) Nehmé, A.; Varadarajan, P.; Sellakumar, G.; Gerhold, M.; Niedner, H.; Zhang, Q.; Lin, X.; Christen, R. D. Modulation of Docetaxel-Induced Apoptosis and Cell Cycle Arrest by All- Trans Retinoic Acid in Prostate Cancer Cells. *Br. J. Cancer* **2001**, *84*, 1571−1576.
(40) Ling, Y. H.; el-Naggar, A. K.; Priebe, W.; Perez-Soler, R. Cell Cycle-Dependent Cytotoxicity, G2/M Phase Arrest, and Disruption of P34cdc2/Cyclin B1 Activity Induced by Doxorubicin in Synchronized P388 Cells. *Mol. Pharmacol.* **1996**.
(41) Mallavadhani, U. V.; Vanga, N. R.; Jeengar, M. K.; Naidu, V. G. M. Synthesis of Novel Ring-A Fused Hybrids of Oleanolic Acid with Capabilities to Arrest Cell Cycle and Induce Apoptosis in Breast Cancer Cells. *Eur. J. Med. Chem.* 2014, DOI: 10.1016/j.ejmech.2013.12.040.

DOI: 10.1021/acsomega.9b02167
ACS Omega 2019, 4, 19614−19622